Synthesis and magnetic properties of polydiphenylamine derivative bearing stable radical groups

Synthesis and Magnetic Properties of Polydiphenylamine Derivative Bearing Stable Radical Groups

Hiromasa Goto[a,b], Hiroshi Ikeda[b,d], Tamotsu Koyano[b,d], Ryozo Yoshizaki[b,d], and Kazuo Akagi[;a,b,c]

[a]Tsukuba Research Center for Interdisciplinary Materials Science (TIMS), [b]Institute of Materials Science, [c]Center for Tsukuba Advanced Research Alliance (TARA), [d]Cryogenic Center, University of Tsukuba, Tsukuba, Ibaraki 305-8573, Japan

Abstract

Poly[4,4'-diphenylamine (3,5-*di-tert*-butyl-4-hydroxy)benzylidene] was synthesized with a dehydrative polycondensation by using H_2SO_4 as a catalyst. After treatment with DDQ, the polymer was oxidized with PbO_2 to generate a stable radical group in the polymer. The colour of the polymer changed from green to dark red upon the oxidation. ESR spectra showed not only a signal with a *g* value of 2.004, but also a so-called "half-field" signal with a *g* value of 4.288.

1. Introduction

Polymer magnetism is one of the most interesting themes in the field of material science [1]. Much effort has been done to increase the spin quantum number in the ground state. Oligo-diphenylcarbenes have been synthesized and showed high ground state, although they were highly chemical active and were only stable in the low temperature range below 150 K [2]. Yoshizawa *et al.* synthesized *poly*(*m*-aniline), and confirmed its ferromagnetic spin order through magnetic susceptibility and electron spin resonance (ESR) measurements. Inter-molecular interaction between the synthetic molecules was found to be ferromagnetic in one stacking orientation [3]. Recently, the chemistry of polyradicals has taken on new aspects in the fields of nano-science and industrial applications. Nishide *et al*. synthesized purely organic high-spin polyradicals and directly confirmed their real nanometer-sized magnetic images using magnetic force microscopy (MFM) [4]. Microcyclic two-strand based polyradical upon calix[4]arene rings was synthesized and its magnetic behavior was elucidated [5]. Non-conjugated polymer having radical groups in the substituents was synthesized and applied as an electrode for a polymer battery [6]. The capacity of the battery using the radical electrode remains unchanged for over 500 cycles of charging and discharging at a high current density. Research in plastic electronics has progressed to not only the synthesis

and application of electrical conducting polymers but also to research on magnetically active polymers.

The spins of the conjugated polymer are expected to be magnetically coupled by through-bond or intermolecular interaction in the polyradical. According to the valence band theory of topological symmetry for the hydrocarbon conjugated skeleton, the ground spin state is described by

$$S = (N^* - N) / 2,$$

where N^* is the number of starred atoms and N is the number of unstarred atoms. It can be predicted that the ground state of this polymer is triplet (following the dimmer model), and that an intramolecular ferromagnetic interaction exists among the π spin centres of this polyradical system [7]. In general, a multi-step procedure is required to synthesize conjugated polymer with radical groups satisfying the spin alignment
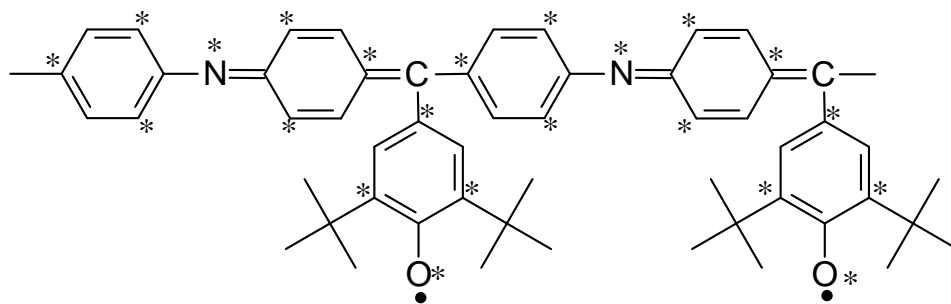
condition, which results in a low total synthetic yield of the desired polymer. Here, we have carried out molecular design of *poly*(4,4'-diphenylamine-3,5-*di-tert*-butoxybenzylidene), and developed a simple and convenient method for the synthesis of the polymer via only three steps.

The radical group in the molecule is essentially unstable, however the neighboring two bulky *tert*-butyl groups protect the phenoxy radical site in this polymer, so the radicals can exist relatively stable. If the distance between the radical substituents is too short, the steric repulsion between the substituents results in a decrease in coplanarity of the polymer main chain. On the other hand, a long distance between the substituents decreases spin-spin interaction between the substituents through the polymer main chain. The distance between the substituents in the polymer that we present in this report may be suitable. In addition, the simple synthetic route and metal-catalyst-free method allows us to avoid contamination of trace amounts of metal in the final polymer.

2. Experimental

2.1 Technique

Infrared spectra (IR) were measured with a JASCO FT-IR 550 spectrometer using

the KBr method. Ultraviolet-visible absorption spectra (UV-Vis) were measured at

room temperature using a HITACHI U-2000 spectrometer with a quartz cell. The

molecular weights of polymers were determined by gel permeation chromatography

(GPC) using a Shodex A-80M column and a JASCO HPLC 870-UV detector, with THF

used as solvent during measurements. ^{1}H NMR spectra were measured with a

BRUKER AM-500 FT-NMR spectrometer (500 MHz). ESR measurements of solid

samples of the polymer were carried out with a JEOL JES TE-200 spectrometer with

100 kHz modulations. The spin concentration was determined using $CuSO_4 \cdot 5H_2O$ as

standard. The sample was packed into a 5 mm quartz tube. The sample tube was

evacuated by a vacuum pump for 3h, and charged with high purity helium gas before

sealing. The spin concentration of the samples was determined by integration of ESR

signals using those of 2,2,6,6-tetramethyl-1-piperidinyloxy (TEMPO) as a standard.

Magnetic susceptibility measurement for the polymer was performed with a Quantum

Design MPMS-7 SQUID magnetometer (± 5 Tesla). The polymer was dissolved in a

chloroform solution of polystyrene, and the solvent was gradually removed by

evacuation to give a powder of the isolated sample. The sample was stuffed into a 5 mm

diameter quartz cell connected to Pyrex glass tube. After evacuation, the tube was

sealed for SQUID measurements. The magnetic susceptibility was measured from 5 to

200 K at a field of 1 T. Inductively coupled plasma analysis (ICP) was carried out with NIPPON JARREL-ASH ICAP-757 emission spectrometer to check the content of transition metal impurities. Ferromagnetic impurities such as Fe, Co, and Ni were confirmed to be less than the lowest limit of the detection. The corrections for the diamagnetism of the quartz cell and polystyrene as diluent were performed by the usual method.

Molecular mechanics (MM) calculations were performed by a Silicon Graphics Cerius^2 system.

2.2 Polymer preparation

All experiments were performed under an argon atmosphere using Schlenk/vacuum line techniques. Tetrahydrofuran (THF), *N,N*-dimetylformamide (DMF), ethanol, acetone, and ether were distilled prior to use. Plastic spatulas and tweezers, and glass pipettes were used instead of metal tools. Diphenylamine and 3,5-di-*tert*-butylhydroxybenzaldehyde were recrystallized from absolute methanol. All flasks were washed with highly purity grade nitric acid, and dried under vacuum before experiments. Polymer synthesis was outlined as shown in Scheme 1. Polymerisations were carried out by dehydrative polycondensation between diphenylamine and aldehyde

group using sulfuric acid as a dehydrating agent [8].

Diphenylamine (5.00 g, 29.5 mmol) and 3,5-di-*tert*-butylhydroxybenzaldehyde (6.92 g, 29.5 mmol) were dissolved in absolute 1,4-dioxane. Sulfuric acid (0.1 ml) was added to the solution very slowly under an argon atmosphere. The reaction mixture was refluxed for 24 h at 90 °C. The solution was poured into a large amount of methanol. Filtration of the solution afforded 4.91 g of *poly* **1** as green solid (yield = 43 %). Subsequently, a solution of *poly* **1** (3.00 g, 7.76 mmol) and 2,3-dichloro-5,6-dicyano-1,4-benzoquinone (DDQ) (5.29 g, 23.3 mmol) in *N*-methyl-2-pyrrolidon (80 ml) was stirred for 12 h at 80 °C. The reaction mixture was poured into a large amount of pure water and filtered to afford 1.92 g of *poly* **2** as dark green polymer (yield = 64 %). A solution of *poly* **2** (1.50 g, 3.90 mmol) and PbO_2 (9.36 g, 39.0 mmol) in chloroform (25 ml) was stirred for 4 h at room temperature. After filtration, the $CHCl_3$ in the filtrate was removed by the freeze drying method to obtain the polyradical *poly* **3** as a dark red solid. *Poly* **3** was immediately charged into an ESR quartz tube for magnetic measurements. All of the polymers are soluble in common organic solvents such as THF and chloroform. The number average molecular weight (M_n) of *poly* **3** was found to be 3500, and the weight average molecular weight (M_w) was 5700, using GPC with a polystyrene standard.

Scheme 1.   Synthetic route for *poly* **3**.

3. Results and Discussion

The IR absorption spectra of *poly* **1** and *poly* **2** are shown in Fig. 1. After DDQ

treatment, the absorption peak around 1500 cm^{-1} corresponding to the C=C stretching

vibration of the benzenoid structure was decreased in intensity, and that at 1590 cm^{-1}

corresponding to the C=C vibration of the quinoid structure was increased in its

intensity. The absorption peak at 1660 cm^{-1} in *poly* **2** was assigned to the C=C

stretching of the methine structure.   The absorption peak at 1330 cm^{-1} was assigned to

C-N stretching in the quinoid structure, since this intensity was increased after DDQ

treatment. These results indicate that the treatment indeed introduced the quinoid

structure to the polymer backbone. Note that although the absorption peak at 1660 cm^{-1},

corresponding to the C=C stretching of the benzenoid structure still remains after the

oxidation (*poly* **2** in Fig. 1), this peak should come from the phenyl ring of the

di-tert-butylphenol. At the same time, the signal at 5 ppm in the ^{1}H NMR spectrum of

poly **1** corresponding to the NH moiety disappeared after DDQ treatment.   This result

suggests that the main chain of *poly* **2** forms a conjugated system.

Fig. 1.   IR absorption spectra of *poly* **1** and *poly* **2**.

UV-Vis absorption spectra of *poly* **1**, *poly* **2**, and *poly* **3** were measured in THF (Fig. 2). The band around 250 nm in all polymer spectra was assigned to the $\pi \rightarrow \pi^*$ transition of the phenylene ring. The band at 445 nm in the *poly* **1** spectra was ascribed to the $\pi \rightarrow \pi^*$ transition of the polymer backbone. This result implies that the conjugated structure was partly formed before oxidation of *poly* **1**. *Poly* **2** showed a peak at 463nm due to the $\pi \rightarrow \pi^*$ transition of the polymer backbone, and *poly* **3** showed a broad absorption band centred at 466 nm, in which the absorption bands of the phenoxy radical moiety and the conjugated polymer backbone are overlapped.

Figure 2.   UV-Vis absorption spectra of the polymers in THF.

The ESR spectra of *poly* **3** were measured at 10–90 K. The polymer showed not only a signal with a *g* value of 2.004, but also a so-called half-field signal with a *g* value of 4.288, as shown in Fig. 3.

Figure 3. ESR spectrum of *poly* **3** at 10 K.

The half-field signal is ascribed to a magnetically forbidden transition ($\Delta M_s = \pm 2$). This implies the existence of multiplet states including a triplet one in the polymer. The temperature dependence of the centre-field signal in ESR spectra is given in Fig. 4.

Figure 4. ESR centre-field signals ($\Delta M_s = \pm 1$) of *poly* **3**.

It is suggested that the multiplet spin state can exist at temperatures up to 90 K. The line shapes of the spectra were unchanged in this temperature range. Next, the distance (*r*) between unpaired electrons was evaluated according to the following equation based on the point dipole approximation,

$$D = 3/2 \ g \ \mu_B \ r^{-3} \ ,$$

where D and μ_B are the fine splitting constant and the Bohr magnetron, respectively. The D value was experimentally determined from the peak-to-peak width of the ESR spectrum ($D = 29.5 \ G$). Thus the value of r was calculated to be 9.9 Å. The MM calculation (twenty monomer repeat units) indicated that in the case where all phenylene

units including the side chains in *poly* **3** are planar, the distance between phenoxy

groups is 10.3 Å; and in the case where the main chain forms a helical structure, the

distance between phenoxy groups is 11.9 Å. This *r* value was found to almost coincide

with the nearest neighboring distance between the phenoxy oxygen atoms, according to

the MM calculations. This indicates that the interaction between the radical spins in the

substituents gives rise to the parallel spin alignment responsible for the multiplet spin

state. Since the magnetic susceptibility (χ) is proportional to the intensity of the ESR

signal, assuming that the line shape is unchanged, χ can be expressed as follows.

$$\chi = C \, \Delta H_{pp}^{2} I_{pp},$$

where ΔH_{pp} is the peak-to-peak line width, I_{pp} is the height of the differential curve, and

C is a constant which depends on the measurement conditions such as sensitivity and

amplitude of the apparatus [9]. As the temperature decreases, χ of *poly* **3** increases, as

shown in Fig. 5. The line width of the signals is constant. The $1/\chi$ vs. T plots for *poly* **3**

(solid sample) estimated by centre field signals (318 mT) is shown in Fig. 5. The plots

obeyed the Currie–Weiss law,

$$\chi T = N_A g^2 \mu_B{}^2 TS(S + 1)/3k_B(T - \theta),$$

where N_A and k_B are Avogadro's number and the Boltzman constant, respectively.

The χT increases as the temperature decreases, but it shows a decrease at 10 K. The

spin concentration was 52 % (3.12×10^{23} spin/mol) per unit cell for ***poly* 3**.

Figure. 5. χ ($\Delta H_{pp}{}^2 I_{pp}$) vs. T and $1/\chi$ [($\Delta H_{pp}{}^2 I_{pp}$)]$^{-1}$] vs. T for ***poly* 3** (estimated from

ESR center field signals of solid sample).

Next we discuss the relationships between the spin concentration and the oxidation

degree and/or the radical amount in the polymer. One can separate oxidation reactions

into two steps, i.e., oxidations by DDQ and by PbO_2. (i) In the first step, the hydrogen

on the amine moiety and that on the methine moiety are eliminated.   The oxidized

polymer is then transformed from a benzenoid structure to a quinonoid one.

Complete oxidation is confirmed by ^{1}H NMR measurement, where the both the amine

proton at 5.0 ppm and the methine proton at 5.6 ppm disappeared after the oxidation.

(ii) Next, the subsequent oxidation by PbO_2 caused hydrogen elimination on the

hydroxy group of *di-tert*-butylphenol. At the same time, one of the lone pair electrons

on the nitrogen atom of the quinoid structure is also eliminated to give a cation radical with an unpaired electron. However, the reaction yield for this third step could not be evaluated. After the oxidation, the degradation and crosslinking of the polymer via radical electrons should have occurred, resulting in a substantial decrease in the spin concentration. This is the reason why the spin concentration is about 50 %, rather than 100 % per unit cell.

The ESR half-field signals are shown in Fig. 6. The half-field signals are due to the inherently forbidden transitions of $\Delta M_s = \pm 2$. The half-field signal gradually decreases in intensity with an increase in temperature from 5 K to 80 K, and then disappears above 80 K. Figure 7 shows the half-field signal intensity of *poly* **3** as a function of $1/T$. The temperature dependent ESR experiment for *poly* **3** gave a linear relation for the doubly integrated intensity of the ESR signal as a function of $1/T$, which is consistent with Curie's law. This result indicates that the triplet state ascribed to the $\Delta M_s = \pm 2$ signal is the ground state, or degeneration of the triplet−singlet state.

Figure 6.   ESR half-field signals of *poly* **3**.

Figure. 7.   Temperature dependence of the ESR signal intensity of the $\Delta M_s = \pm 2$

transition of ***poly* 3** (solid).

A $1/\chi$ vs. *T* plot based on the SQUID results for *poly* **3** is shown in Fig. 8. The results

suggested that *poly* **3** exhibits an antiferromagnetic interaction owing to an interchain

interaction ($\theta = -1.5$ K). This duality may be due to the coexistence of ferromagnetic

intrachain interactions and antiferromagnetic interchain interactions in the polymer.

Namely, the parallel spin alignment is constructed by way of through-space interactions

between the phenoxy radicals. At the same time, however, the mutual interactions of the

ferromagnetic polymer chains result in antiferromagnetic nature. This is because the

polymers are randomly oriented from a macroscopic viewpoint, which is typical of

common polymers.

Figure. 8. $1/\chi$ of ***poly* 3** as a function of *T* in low temperature region (estimated from

SQUID).

4. Conclusions

We developed a simple and convenient method for the synthesis of a polydiphenylamine

derivative bearing a phenoxy radical group. Although SQUID measurement indicated

that the polymer, as a whole, behaves as an antiferromagnetic material due to interchain interactions, the half-field signal ($\Delta M_s = \pm 2$) was observed below 80 K in the ESR spectra. It was determined from analysis that the ferromagnetic interaction exists between the phenoxy radicals in the substituents.

Acknowledgments

References

[1](a) Miura Y, Ushitani Y, Inui K, Takei Y, Takaku T, Ito K. Macromolecules 1993;26:3698. (b) Kaneko T, Toriu S, Kuzumaki Y. Nishide H, Tsuchida E, Chem Lett 1994:2135. (c) Yoshioka N, Lahti PM, Kaneko T, Kuzumaki Y, Tsuchida E, Nishide H. J

Org. Chem 1994;59:4272; (d) Nishide H, Kaneko T, Nii T, Katoh K, Tsuchida E, Lahti PM. J Am Chem Soc.1996;118:9695 (e) Miura Y, Ushitani Y. Macromolecules 1993;26:7079 (f) Goto H, Akagi K, Shirakawa H, Synth. Met.1997; 85:1683. (g) Pu, YJ, Soma M, Tsuchida E, Nishide H. J Polym Sci Part A: Polym Chem 2000;38:4119. (h) Miyasaka M,Yamazaki T, Tsuchida E, Nishide H. Macromolecules 2000;33:8211. (i) Kaneko T, Matsubara T, Aoki T. Chem Mat 2002;14:3898. (j) Kaneko T. Makino T, Miyaji H, Teraguchi M, Aoki T, Miyasaka M, Nishide H. J Am Chem Soc 2003;125:3554. (k) Fischer G, Mann C, Pilawa B, Pongs B. Synth Met 2003;137:1193. (l) Kaneko T, Tatsumi H, Aoki T, Oikawa E, Yoshiki H, Yoshioka N, Tsuchida E, Nishide, H. J Polym Sci Part A: Polym Chem Ed. 1999;37:189. (m) Pascale W, Philippe T, Jacques LM. Synthesis 2002:1286. (n) Adam W, Maas W. J Org Chem 2000;65:7650. (o) Lahti PM, Inceli AL, Rossitto FC. J Polym Sci Part A: Polym Chem 1997;35:2167. (p) Takahashi M, Nasu Y, Nishide H, Tsuchida E. Polym J 1999;31:203. (q) Kaneko T, Takahisa M, Miyaji H, Onuma A, Teraguchi M, Aoki T. Polyhedron 2003;22:1845.

[2] (a) Itoh K. Pure Appl Chem1978;50:1251. (b) Iwamura H. Pure Appl Chem 1986;58:187. (c)Sugawara T, Bandow S, Kimura K, Iwamura H, Itoh K. J Am Chem Soc 1986;108:368.

[3] (a)Yoshizawa K, Tanaka K, Yamabe T, Yamaguchi J. J Chem Phys 1992;96:5516.

(b) Yoshizawa K, Tanaka K, Yamabe T, Yamaguchi J. Chem Lett 1990:1311. (c) Yoshizawa K, Ito A, Tanaka K, Yamabe T, Solid State Comm. 1993; 87:935.

[4] (a) Miyasaka M, SaitoY, Nishide H. Adv Functional Mat 2003;13:113. (b) Miyasaka M, Yamazaki T, Tsuchida E, Nishide H. Polyhedron 2001;20:1157.

[5] Rajca A. Lu K, Rajca S. J Am Chem Soc 1997;119:10335.

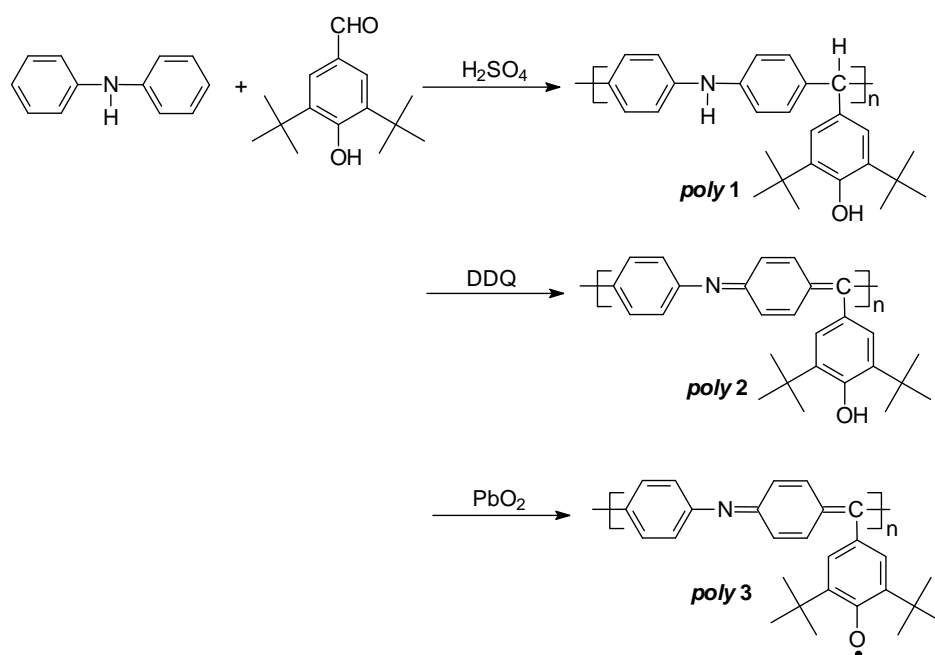[6] Nakahara K, Iwasa S, Satoh M, Morioka Y, Iriyama J, Suguro M, Hasegawa E. Chem Phys Lett 2002; 359: 351.

[7] (a) Ovchinnikov A, Theor Chim Acta 1978;297:47. (b) Klein DJ, Nelin CJ, Alexander S, Matsen FA. J Chem Phys 1982;77:3101.

[8] Chen WC, Jenekhe SA. Macromolecules 1992;25:5919.

[9] The Chemical Society Japan Ed. Jikkenkagaku Koza (Lectures of Chemical Experiments), Maruzen, Tokyo 1967;13.

Scheme 1. Synthetic route for *poly* **3**.

Figure. 1. IR absorption spectra of *poly* **1** and *poly* **2**.
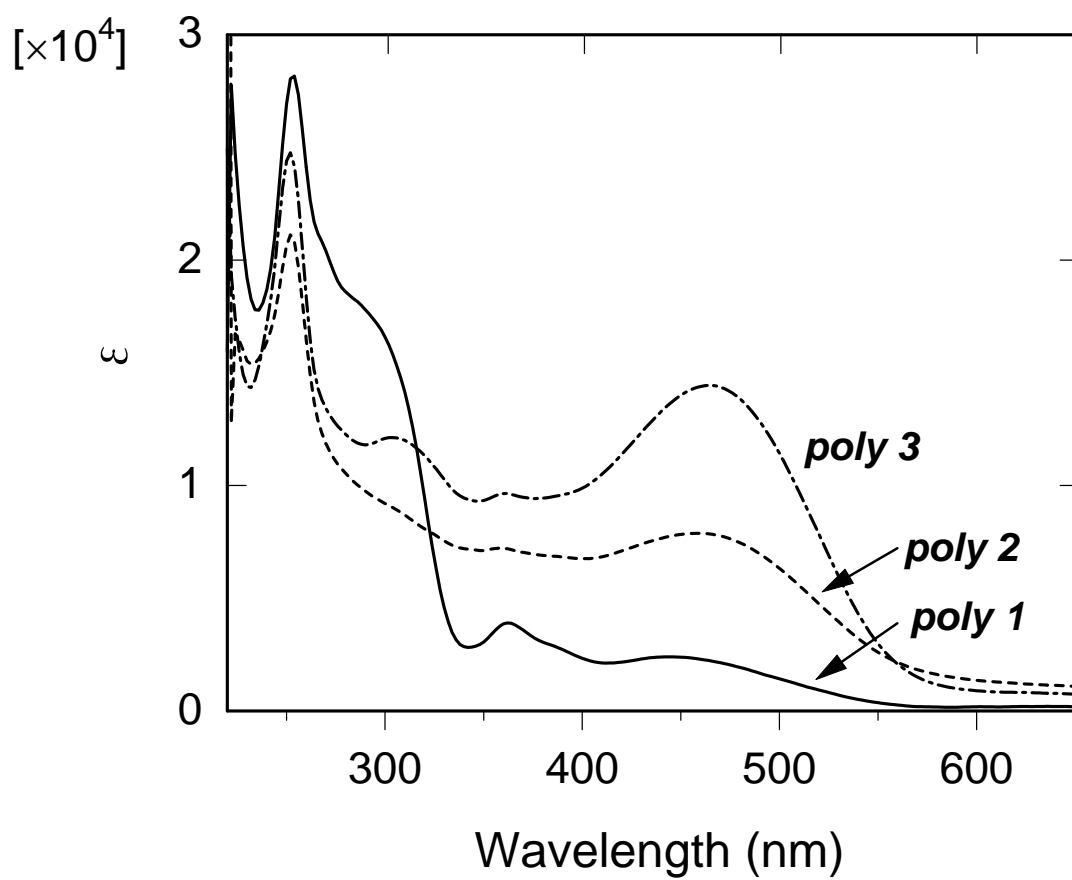
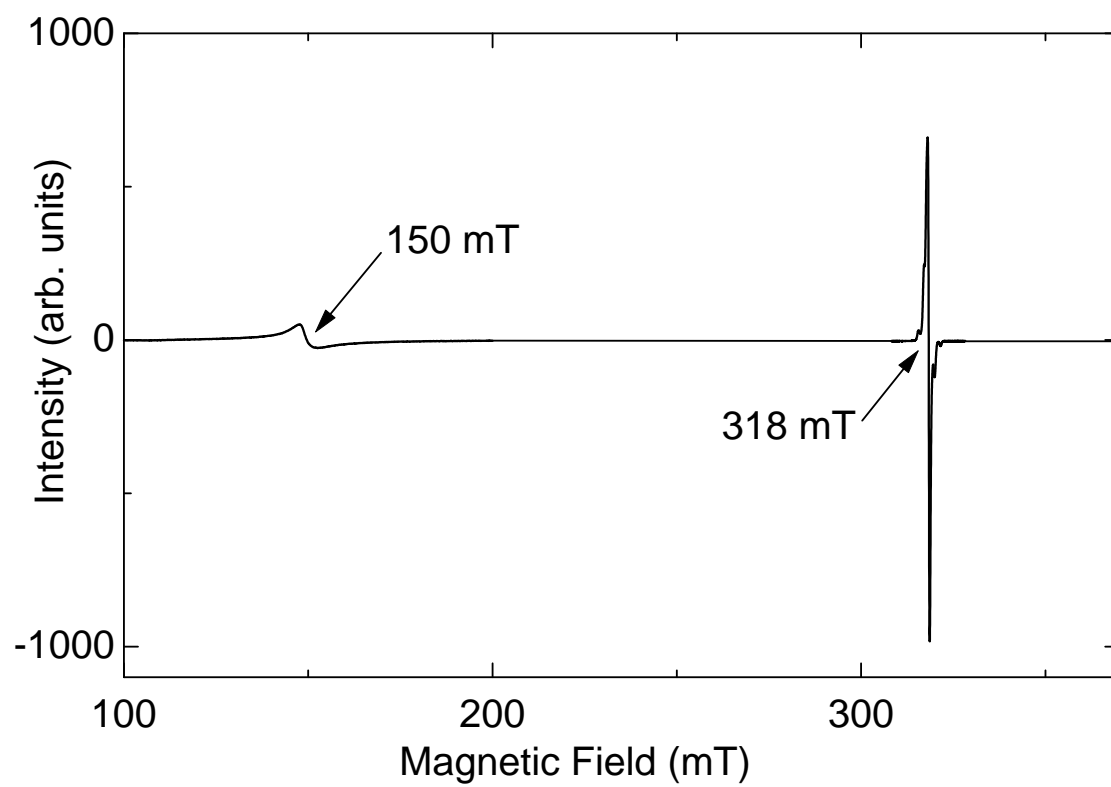Figure. 2.   UV-Vis absorption spectra of the polymers in THF.
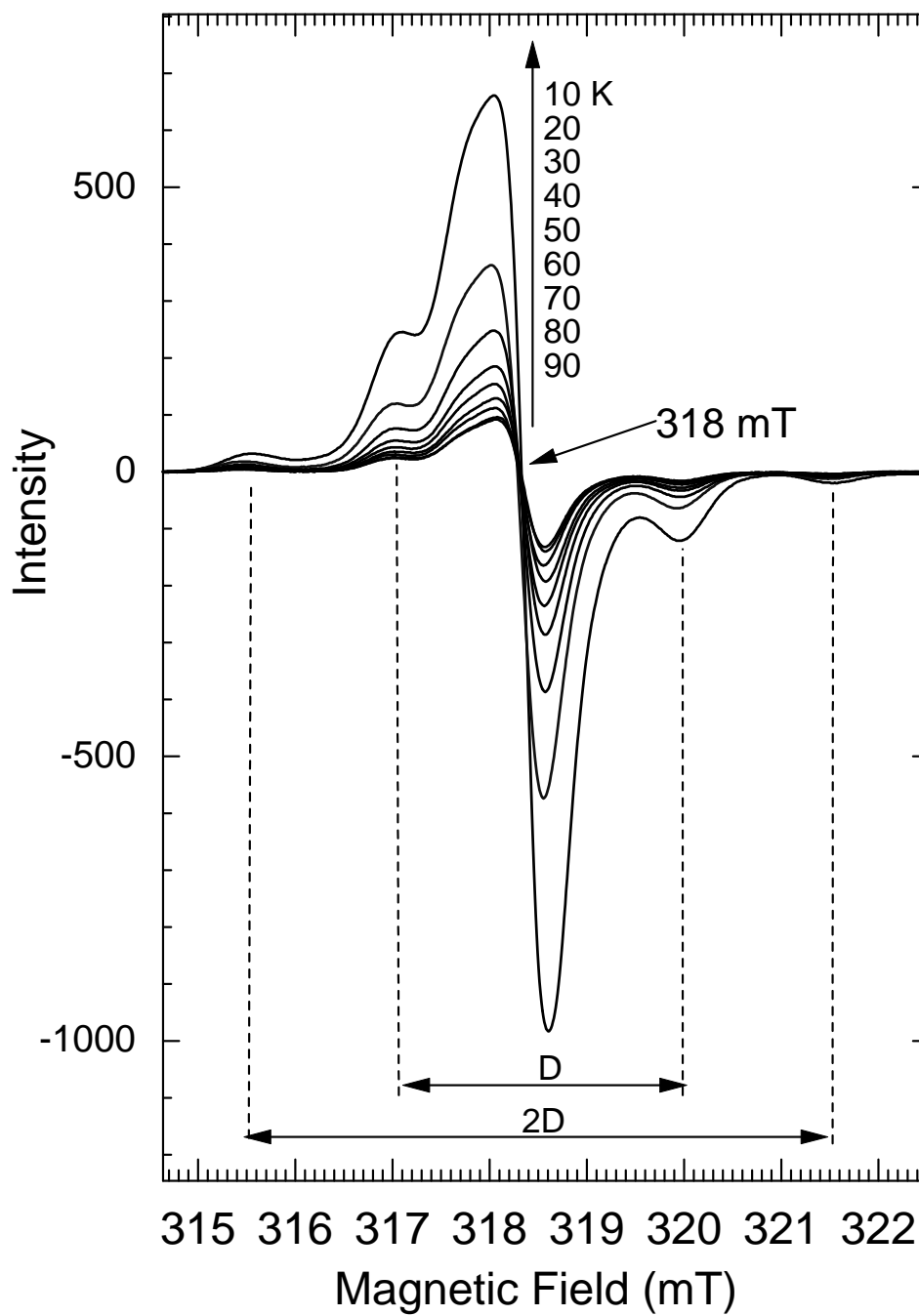
Figure 3.   ESR spectrum of *poly* **3** at 10K.

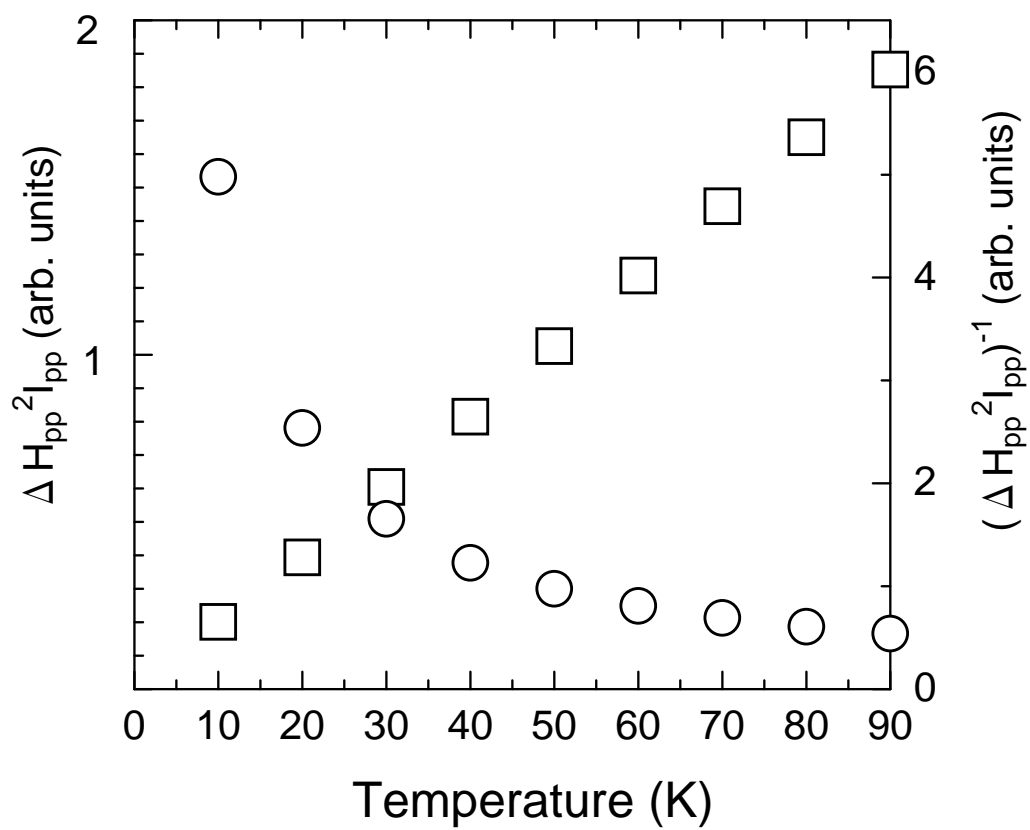Figure 4.   ESR centre-field signals ($\Delta M_s = \pm 1$) of *poly* **3**.

Figure. 5. χ ($\Delta H_{pp}{}^2 I_{pp}$) vs. T and $1/\chi$ [($\Delta H_{pp}{}^2 I_{pp}$)]$^{-1}$] vs. T for **poly 3** (estimated from ESR centre field signals of solid sample).
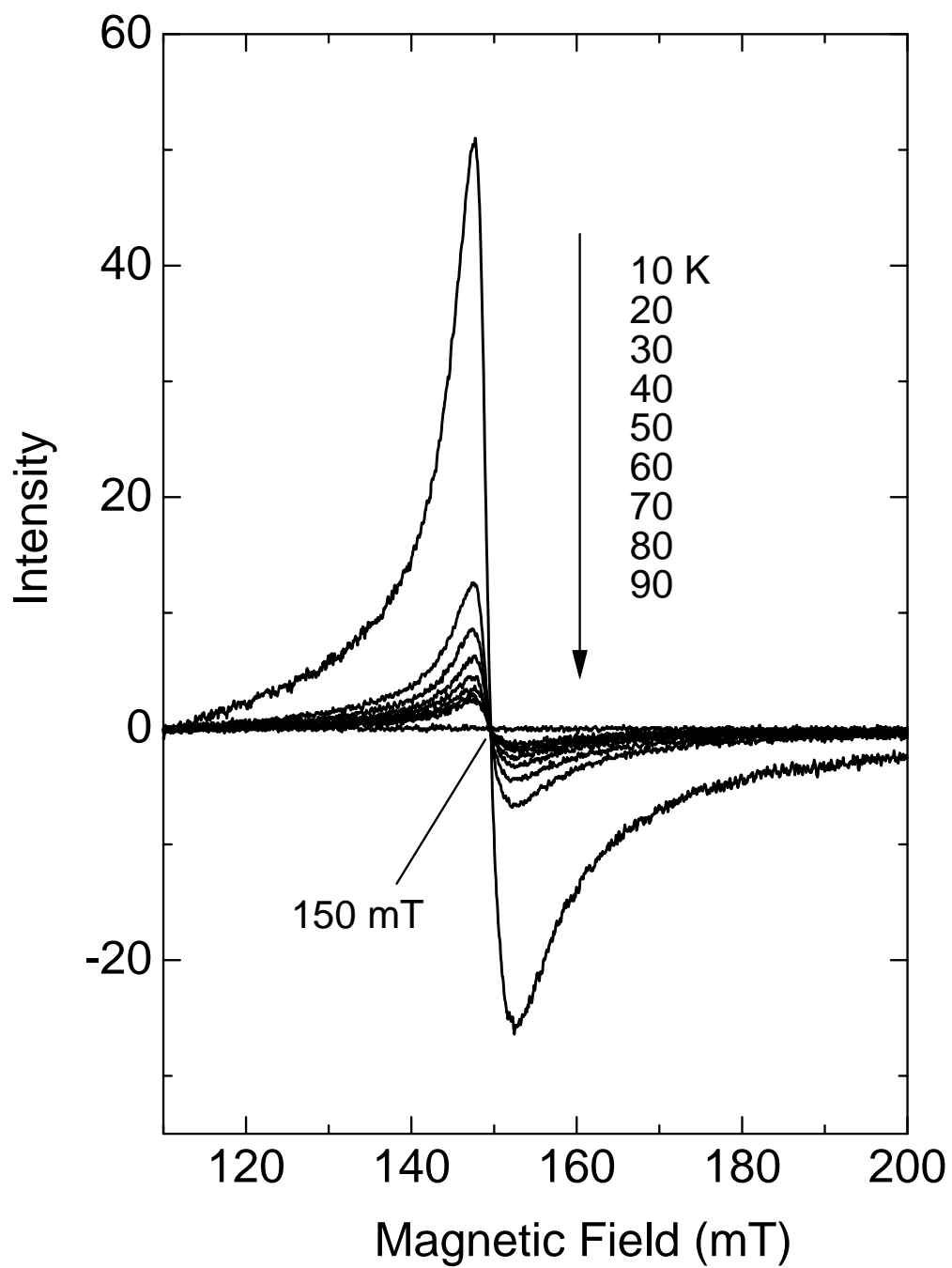
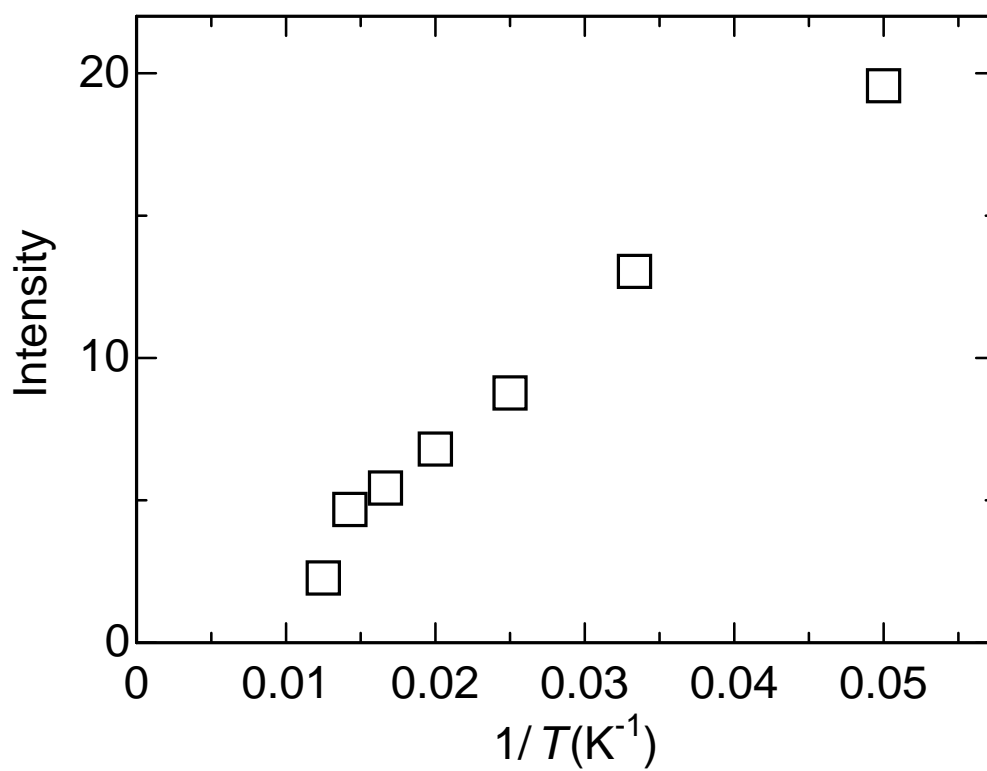Figure 6. ESR half-field signals of *poly* **3**.

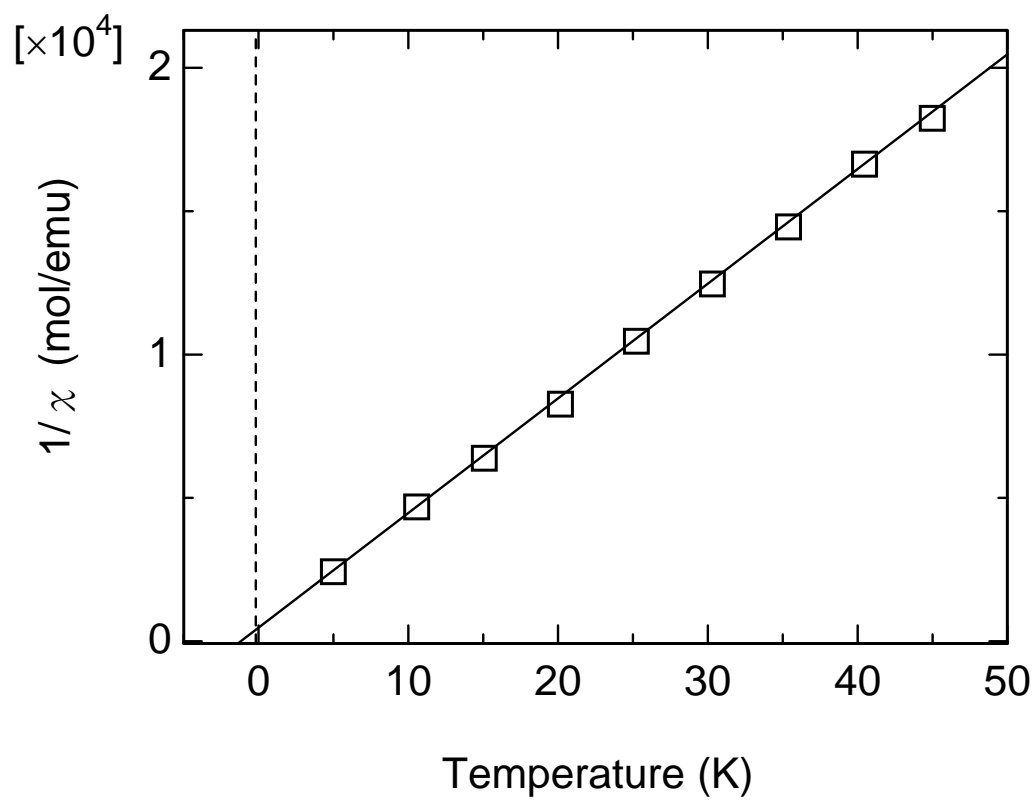Figure 7. Temperature dependence of the ESR signal intensity of the $\Delta M_s = \pm 2$ transition of *poly* **3** (solid).

Figure. 8. $1/\chi$ of *poly* **3** as a function of *T* in low temperature region (estimated from

SQUID).

Figure Captions

Scheme 1.   Synthesis route for *poly* **3**.

Figure 1.   IR absorption spectra of *poly* **1** and *poly* **2**.

Figure 2.   UV-Vis absorption spectra of the polymers in THF.

Figure 3.   ESR spectrum of *poly* **3** at 10 K.

Figure 4.   ESR centre-field signals ($\Delta M_s = \pm 1$) of *poly* **3**.

Figure. 5. χ ($\Delta H_{pp}{}^2 I_{pp}$) vs. *T* and $1/\chi$ $[(\Delta H_{pp}{}^2 I_{pp})]^{-1}]$ vs. *T* for *poly* **3** (estimated from ESR centre field signals of solid sample).

Figure 6.   ESR half-field signals of *poly* **3**.

Figure 7.   Temperature dependence of the ESR signal intensity of the $\Delta M_s = \pm 2$ transition of *poly* **3** (solid).

Figure. 8. $1/\chi$ of *poly* **3** as a function of *T* in low temperature region (estimated from SQUID).